DESIGN OF A MEMBRANE APERTURE DEPLOYABLE STRUCTURE*

J. Enders [1], S. Kas-Danouche [2], W. Liao [3], B. Rasmussen [4], T. Anh Vo [5], K. Yokley [6]
L. Robertson [7] and R.C. Smith [6,8]

Abstract

Ultra-lightweight, membrane primary mirrors offer a promising future for space telescope technology. However, the advantages of the lightweight structure of the mirrors are restricted by an extremely high susceptibility to microyield. Hence, careful packaging of the membranes is required when transporting mirrors of this type into space. Four packaging models, a cylindrical roll, an umbrella model, a multi-cut model and a single cut model, are presented and compared with each other. Factors such as curvature of the compressed membrane, stability after deployment, and the size of the launch vehicle are considered. All four packaging models appear to be feasible with certain materials and hence warrant physical testing.

Introduction

As described in [2], there have been dramatic improvements in technologies and concepts for large telescopes for both ground and space applications. However, the act of launching objects into space poses specific constraints on the structure and deployment of the cargo transported. Due to the high launch cost, ultra-lightweight, membrane primary mirrors have long been sought after by both NASA and the Department of Defense as a technology that could realize large aperture systems with low areal densities. Research on membrane structures has culminated in the fabrication of meter-class lightweight structures with optical quality surfaces. These membranes are 10-100 microns thick and have surface qualities usable in visible spectrum applications. However, the available structures that provide boundary support are so heavy that they eliminate the benefit derived from such lightweight apertures. Since these membranes must maintain an extremely high surface quality after release into space, the membranes cannot be packaged in ways that deform their shape outside an extremely small acceptable range. Thus, many factors must be taken into consideration when developing strategies for folding the membranes.

A sketch of a prototypical telescope is depicted in Figure 1. As diameter length of the primary mirror increases, so does its power of resolution. Currently, the size of such telescopes has been bounded by the size of the launch vehicle. More recently, however, researchers have begun to consider ideas regarding packaging methods that would enable the compactification of much larger mirrors without creating damage beyond desired accuracy. In order to attain the successful packaging of a large mirror, one must carefully consider the size of such an aperture, the size of the launch vehicle, the ease of deployment of the membrane into space, stability, the curvature of the folding method, as well as the allowable deformation of the material after being compacted.

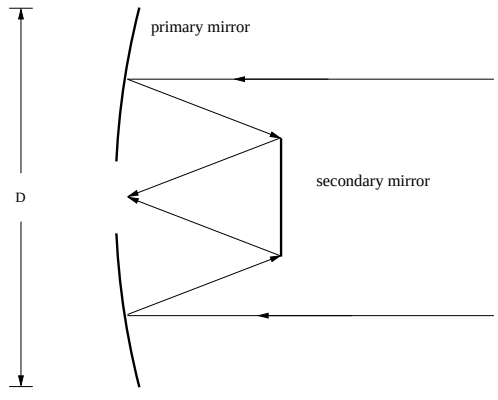

Figure 1: Schematic representation of membrane mirror system.

* This problem was investigated by the first six authors under the direction of the last two authors during the Industrial Mathematics Modeling Workshop for Graduate Students held at North Carolina State University on July 22-July 30, 2002.

[1] Michigan State University
[2] N.J. Inst. of Tech.; Univer. de Oriente, Venezuela
[3] Mississippi State University
[4] Georgia Institute of Technology
[5] California State University Fullerton
[6] North Carolina State University
[7] US Air Force Research Lab, Kirtland AFB
[8] Center for Research in Scientific Computation

Four different compacting schemes are considered in the following analysis. These schemes include folding arrangements for an uncut aperture as well as arrangements that require cutting the aperture at certain places. The radius of curvature necessary for each folding will be evaluated and compared to the minimum radius of curvature allowed by potential aperture materials.

Cylindrical Roll

As stated previously, one goal of any membrane folding is to assure that it fits into the launch vehicle. In subsequent discussion, two ways to compress the membrane without cutting it are developed while noting that control of the maximal curvature is necessary.

The usable surface of the membrane also cannot be too small in order to guarantee a good resolution. The mathematical tool to compute whether the effective size of a membrane is sufficiently big is based on the Modulation Transfer Function (MTF). Consider the doubly curved membrane as depicted in Figure 2. Let D denote the diameter of the aperture when projected into the $xy-$plane, and let d be the diameter of the hole in the membrane. If a matrix M is defined to have an entry of one wherever there is membrane material and zero elsewhere, the resulting Autocorrelation Function computes the convolution of M with itself. Dividing this matrix by the number of ones in M yields the MTF of M. If the MTF value at a point inside the perimeter of the original shape falls below 20%, it becomes difficult or even impossible to resolve certain objects. In Figure 3, values under 20% are black. Once those parts intrude into the black circle representing the size of the disk, the size of the surface is too small.

In the case of the washer, d needs to be smaller than approximately $0.5D$ in order for the mirror to have a sufficient resolution. (Remark: In Figure 3 and later figures of the MTF, only the center part of the MTF matrix, which is the relevant part, is plotted.)

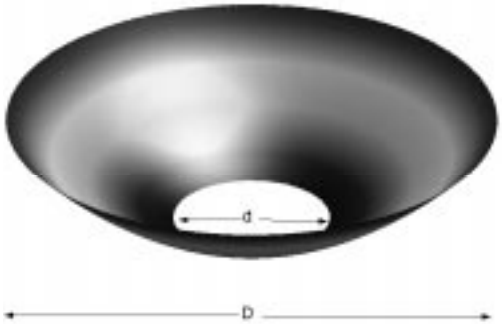

Figure 2: Doubly curved membrane.

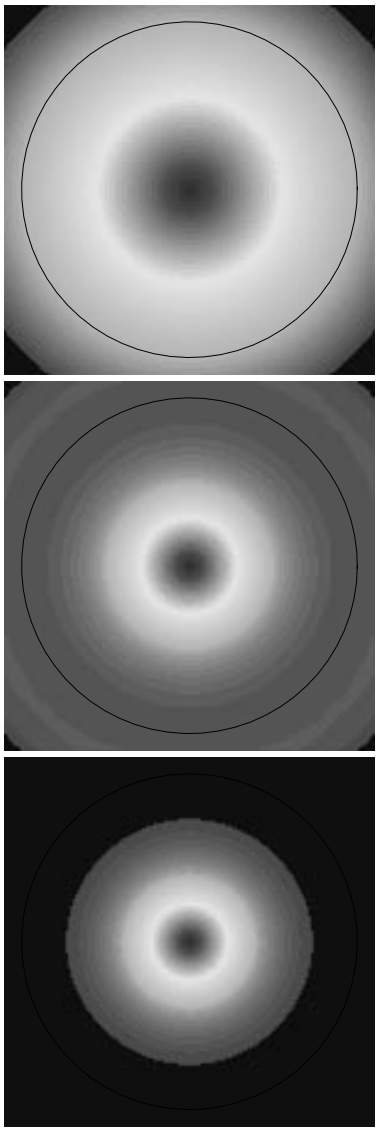

Figure 3: The MTF of the membrane matrix M for $d = 0.1D$, $d = 0.5D$, and $d = 0.6D$.

Since the optimization of the total aperture weight is also desirable, the maximum d (i.e., $d \approx 0.5D$) is used in this and most of the other sections. However, one might want to go with a smaller d in order to increase stability.

When trying to find a way to package the membrane in the launch vehicle, probably the most straightforward idea is to roll the membrane once as depicted in Figure 4. If the membrane was flat, pulling two opposite sides of the aperture together

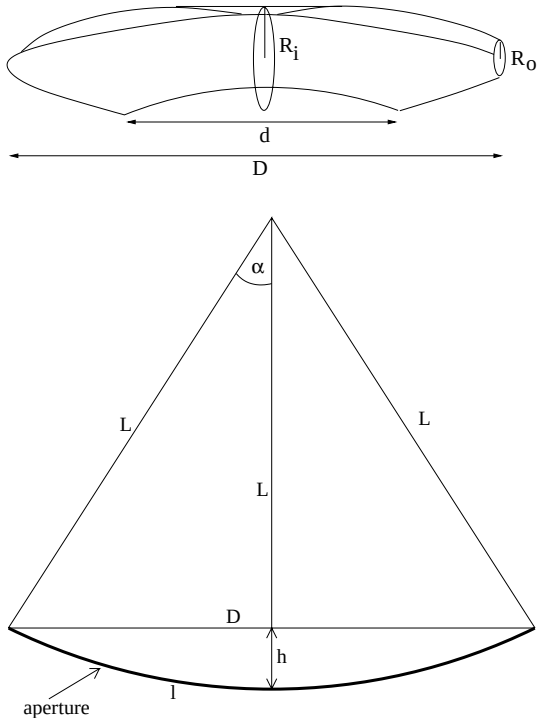

Figure 4: Cylindrical roll and geometry for computing the different radii of curvature of the cylindrical roll.

would result in a cylindrical roll. In reality a more complicated shape would result because the mirror is doubly curved. Computation of the the maximal radius of curvature for this cylindrical roll begins by considering the radius R_i of the inner circle.

Assume that the aperture can be looked viewed as a circle, even if, in fact, it has a parabolic shape. This is reasonable as long as the radius of curvature L of the mirror is much bigger than its diameter D. From Figure 4 it follows that

$$\alpha = \sin^{-1}\left(\frac{D}{2L}\right).$$

Therefore the arc length once across the membrane is

$$\ell = 2\alpha L$$

and hence

$$R_i = \frac{\alpha L}{\pi} = \frac{L}{\pi}\sin^{-1}\left(\frac{D}{2L}\right). \qquad (1)$$

From Figure 4, one can see that when rolling the membrane, the outer radius of curvature R_o is bounded below by

$$R_o \geq R_i - h$$

where

$$h = L - \sqrt{L^2 - \frac{D^2}{4}}.$$

Therefore the largest curvature will occur at the outside of the roll. Hence, for the minimal radius of curvature $R_f = \min\{R_o, R_i\} = R_o$ of the cylindrical roll, the estimate

$$R_F \geq \frac{L}{\pi}\sin^{-1}\left(\frac{D}{2L}\right) - L + \sqrt{L^2 - \frac{D^2}{4}} \qquad (2)$$

holds. Since the material can only sustain a limited curvature due to optical constraints, (2) sets bounds on L and D.

Finally, consider the constraint that the folded membrane has to fit into the rocket, and let R_{rocket} be the radius of the rocket. It follows that if the cylindrical roll is in an upright position, this condition is satisfied if

$$R_{rocket} \geq R_i = \frac{L}{\pi}\sin^{-1}\left(\frac{D}{2L}\right). \qquad (3)$$

Clearly the height of the roll is given by D.

For example, if a rocket has a radius $R_{rocket} = 2$ m and the mirror has a radius of curvature $L = 20$ m, then a membrane mirror of 12.3 m can be packaged as a cylindrical roll.

Umbrella Design

The umbrella design, while one of the easiest to assemble, is also one of the least compact. Simply put, this design is a doubly-curved washer, folded down an axis through the center like an umbrella. The only action required to unfurl it is a one-dimensional slide along a rod. Like the cylindrical roll, the umbrella design requires no cuts of the material and can therefore tolerate a large inner diameter while maintaining a sufficiently MTF.

Of course, there is no canonical way to fold a circular, doubly curved washer along the inner wall of a cylinder, so this design requires a choice of folding patterns. The following discussion is an analysis of one particular – and particularly straightforward – choice of folding geometry, but others may be more efficient.

Figure 5(a) shows a cross-section of the folded mirror with the proposed folding geometry. It is a set of nine circles arranged in a ring, with nine circles on the outside of the ring. As discussed below, this design may accommodate more or fewer circles, depending on the compactness requirements. The folded mirror weaves through the circles in a natural pattern, as indicated by the solid lines. Figure 6

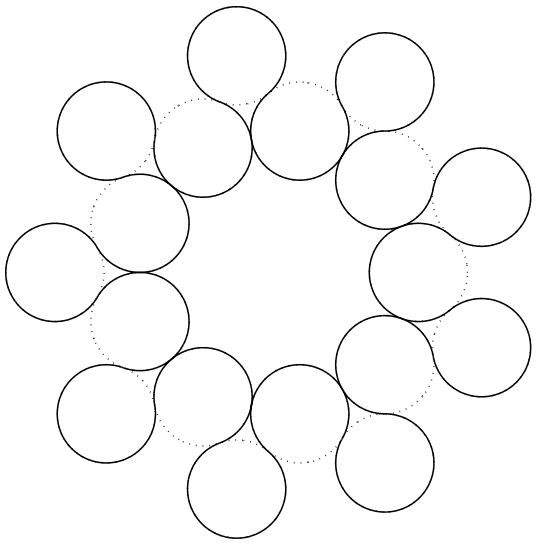

(a)

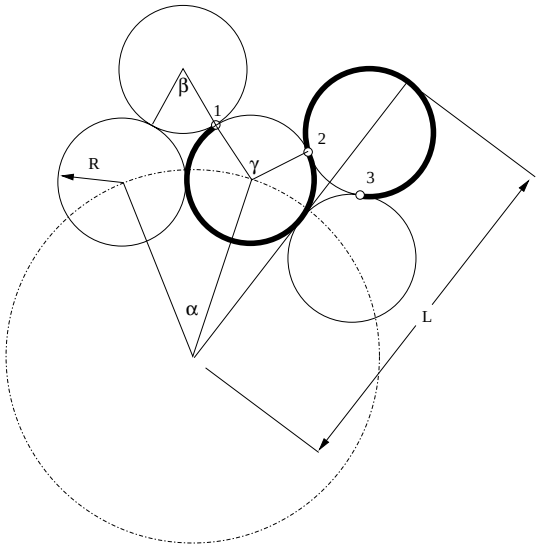

(b)

Figure 5: (a) Cross-section of the folded umbrella, and (b) geometry of the folded umbrella.

shows a diagram of a full, three-dimensional, compressed mirror.

The use of circles in the folding pattern makes the overall shape easy to analyze. Figure 5(b) shows an expanded region of a cross section of the folded design. Let N be the total number of circles in either the inner or outer ring, and let D, d, and R_{rocket} be defined as in the previous section. Trigonometric computations then yield the angles and lengths

$$\alpha = \frac{2\pi}{N} \tag{4}$$

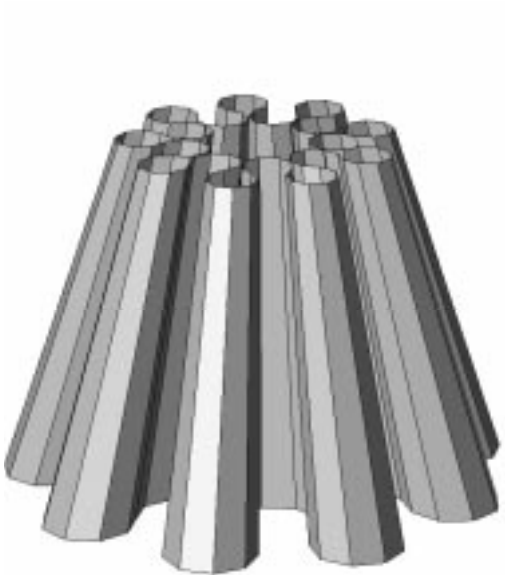

Figure 6: The folded umbrella design.

$$\beta = \frac{5\pi}{3} \tag{5}$$

$$\gamma = \pi\left(\frac{1}{3}+\frac{2}{N}\right) \tag{6}$$

$$L = R\left(1+\sqrt{3}+\cot\frac{\pi}{N}\right). \tag{7}$$

Thus, the arc length from point 1 to point 2 is $\pi R\,(5/3-2/N)$ and the arc length from point 2 to point 3 is $5\pi R/3$. The total arc length is

$$s = N\pi R\left(\frac{10}{3}-\frac{2}{N}\right). \tag{8}$$

The number of folds, N, should be as small as possible in order to keep the minimum radius of curvature, R_F, as large as possible.

Two geometrical constraints determine the minimum N. First, the total arc length at the bottom (i.e., the widest part) of the umbrella must be πD. Second, the folded design must fit inside a payload bay with radius, R_{rocket}, so $L \le R_{rocket}$, again at the bottom of the umbrella. The constraints, together with (7) and (8), show that N must be large enough to satisfy

$$R_{rocket} \ge \frac{D\left(1+\sqrt{3}+\cot(\pi/N)\right)}{(10N/3-2)}. \tag{9}$$

In order to support the membrane properly, N should be at least 5, but this does not usually constrain the design, since the size of the payload bay dictates that there be at least 8-9 folds in most cases.

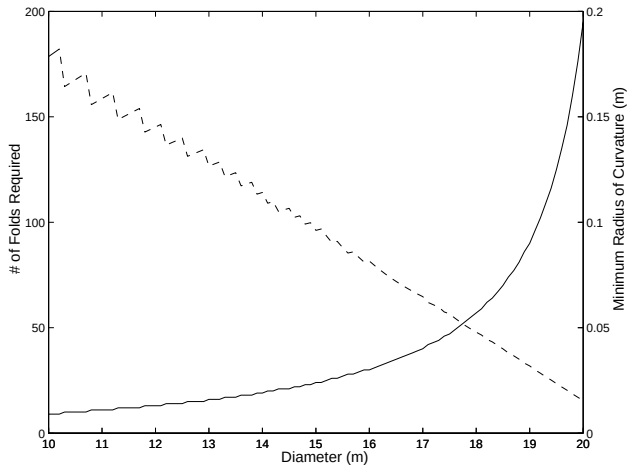

Figure 7: Design parameters versus D.

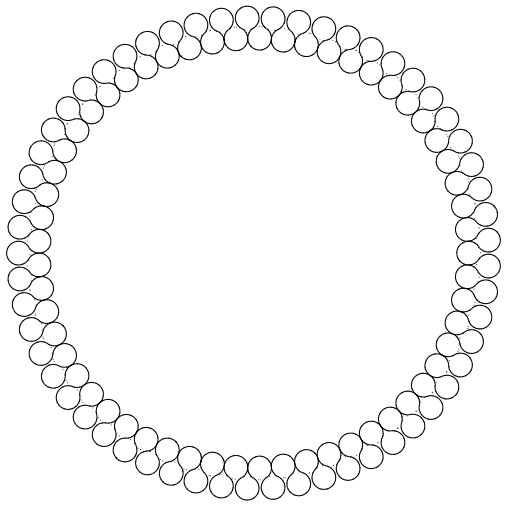

Figure 8: Failure of the circular folding pattern.

The total arc length on top is πd, so (8) gives the minimum radius of curvature

$$R_F = \frac{d}{(10N/3 - 2)}. \tag{10}$$

In summary, the design algorithm for the folding umbrella can be summarized as follows:

- Start with a given D and R_{rocket}. Choose d to be as large as possible while still satisfying the required optical properties (usually $d \approx 0.5D$).
- Use (9) to compute the minimum N required to fit the umbrella into the payload bay.
- Use (10) to compute the minimum radius of curvature at the top.
- This will dictate the material composition and maximum thickness of the membrane.

Figure 7 shows the behavior of N and R_F as functions of D for $d = 0.5D$ and $R_{rocket} = 2$ m.

Clearly, the number of folds becomes too large and the minimum radius becomes too small as D grows above 15 m. The reason for this is that the design uses only *circular* folds, whereas other choices might be more efficient in other situations.

Figure 8, for example, shows a cross section at the bottom of the umbrella for $R_{rocket} = 2$ and $D = 18$, which together force $N = 57$. The circular folds in this case are obviously inadequate, since the center of the cross section is an large open space with no material, while the folds form a highly twisted perimeter.

Therefore, for larger mirrors, other choices of folding patterns besides circles – such as stacking more layers of circles, using ellipses, etc., – are superior. As the folding patterns become more complicated, analysis of the design becomes more difficult.

Nonfeasible Pattern

To illustrate the possibility of other folding patterns, consider one choice that turns out to be inadequate. Let r_o, p, and θ be a fixed radius, a fixed integer, and an angular coordinate, respectively. Define a cross-section of the umbrella as the image of a parameterized curve given in radial coordinates by

$$\mathbf{x}(\theta) = (r_0 + \rho \sin(p\theta), \theta). \tag{11}$$

The sine function applied along a circle becomes very sharp near the origin, thus inciting an unacceptably small radius of curvature. For example, consider $R_{rocket} = 2$ and $D = 10$, with $p = 10$. Then setting $r_0 = 1.25$ at the bottom of the umbrella seems reasonable. The total arclength of the cross-sectional curve must be πD, which leads to a value of $\rho = 0.74$.

Figure 9 illustrates what happens next. A ring on the outside indicates the dimension of the payload bay, and the inner curve is the wrapping pattern. As illustrated in the figure, the minimum radius of curvature that occurs nearest the origin is untenable. In fact, it has a closed-form representation

$$R_{min,curve} = \min\left\{ \frac{(r_0+\rho)^2}{r_0+\rho+\rho p^2} \ , \ \frac{(r_0-\rho)^2}{r_0-\rho-\rho p^2} \right\}.$$

The minimum radius of curvature of the parametric curve with the given values is about 0.035 m which is too small for most materials.

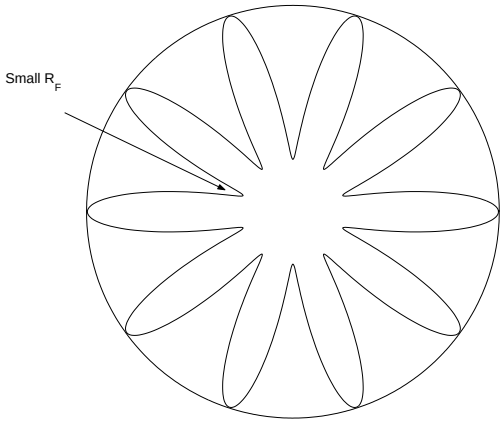

Figure 9: Parametric sine folding pattern.

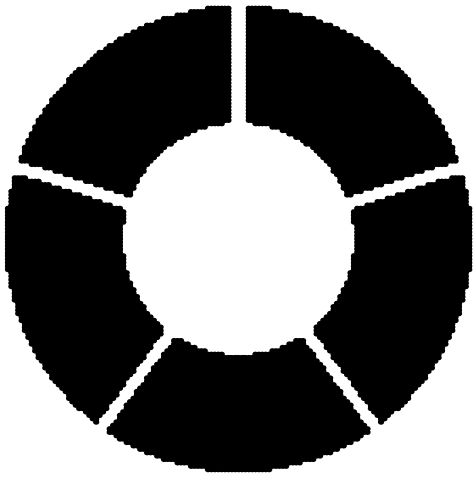

Figure 10: The multi-cut mirror with $N = 5$.

Multi-Cut Model

We consider here the analysis of a model which consists of dividing the membrane in N parts and then rolling them so that they can fit inside the launch vehicle.

Analysis of Single Component

The multi-cut configuration is illustrated in Figure 10. Here N cuts are made along a diameter of the lens, from the outer disk to the inner one. This particular configuration allows an excellent original-to-packaged compression ratio, and thus larger lens would fit into current launch vehicles. The analysis of this configuration is not complicated and begins by reducing the three-dimensional lens down to a two-dimensional circle. This simplifying assumption is reasonable since the original three-dimensional lens curvature is low for telescope and focusing mirror applications.

As shown in Figure 10 and Figure 11, after a cut is made, the piece is rolled along chord S to form a shape that is circular near its bottom but somewhat parabolic at the top. The whole folded piece now looks like a cylinder with a diagonal part removed. The top portion will naturally go into a state of lowest energy, and the implication is that the curvature of the top is not high enough to cause concern. The bottom circle is where greatest curvature K_b will occur. This K_b can be expressed as

$$S = 2\pi R_b = D\sin(\pi/N)$$

$$R_b = \frac{D}{2\pi}\sin(\pi/N)$$

$$K_b = \frac{1}{R_b} = \frac{2\pi}{D\sin(\pi/N)},$$

where $N > 1$, and K_b is the curvature value at the bottom of the rolled up piece.

Since natural stability of the lens after deployment is a consideration, a large value of N would not be advantageous in that regard. However, cutting the lens into a large number of pieces does have its merit. When N goes past a certain value, pieces no longer need to be rolled for them to fit into the launch vehicle, and therefore curvature is no longer a consideration. For this particular configuration, a relatively small N in the range of three to eight was considered. Values of R_b for different N are summarized in Table 1.

Regarding the criterion concerning the modulation transfer function (MTF), Figure 12 shows that our lens achieves an overall value of 20% or better. Stability of the multi-cut model is questionable, but discussion of the natural frequencies of the mirror

Table 1: Radius of curvature R_b of each piece for different values of N (the number of pieces) and D (the aperture diameter).

N	R_b for $D = 10$	R_b for $D = 20$
2	1.591549	3.183099
3	1.378322	2.756644
4	1.125395	2.250791
5	0.935489	1.870979
6	0.795775	1.591549
7	0.690547	1.381095
8	0.609059	1.218119

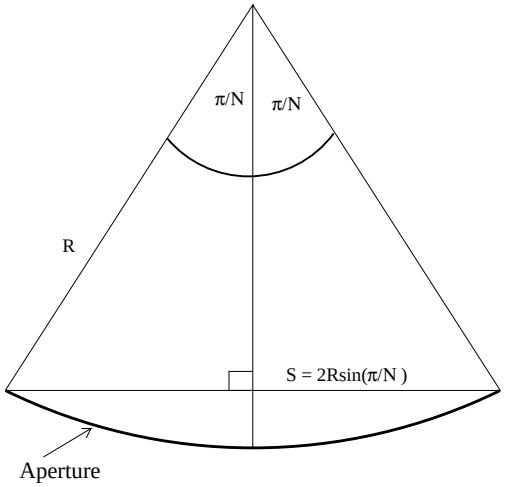

Figure 11: A single piece of the multi-cut mirror, viewed flat.

will not be presented here. To insure maximum stability for the multi-cut configuration, set the thickness t of the material as high as possible. Curvature restraints dependent on thickness are contained in the next section.

Packing and Deployment Procedure

The last subsection contained an analysis of each piece of the membrane, and the radius of curvature versus the maximum curvature of the material and the rocket radius can be used to decide the number of cuts to make in each membrane. Here, steps required in the packing and deployment procedure for the multi-cut model are summarized.

First the membrane is cut into N parts. Each part has a mechanism attached which acts as a sliding track. This will allow each membrane part to slide over the one next to it. This action is very similar to the mechanism used in sliding door closets. A string which connects and keeps all parts together goes through the holes on top of each sliding track. One part slides on top of the next one, this set of two parts slides on top of the next part, and so on in successive process until all parts are in one stack.

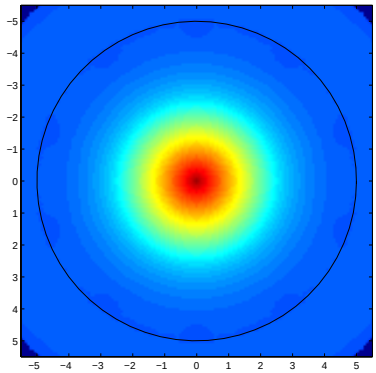

Figure 12: The MTF of the multi-cut mirror

In the next step the membrane parts are rolled from top to bottom in such a way that the outer corners of the first part (on top) will touch each other, almost forming a cylinder. Next the other pieces roll around the first piece in a similar fashion.

A concern which arises in the process of packaging is the following: the curvature of the most inner rolled part must satisfy the maximum curvature criteria, and the radius of curvature of the outermost rolled part must be less than the rocket radius.

In order to recover the original membrane, the unfolding proceeds in reverse manner: all the parts unroll and each part slides in the opposite direction as in the original packaging process. Finally, the string will tighten the separate pieces together.

Single Cut Model

Cutting the disk in one place and then rolling the resulting strip around itself is another folding possibility. The single cut in the membrane can be described as a small width removed radially from the circle when evaluating the MTF, and the resulting information can be used to determine the largest usable diameter d for the hole in the center of the mirror. Using the largest possible d will help lower the radius of curvature of rolling the mirror around itself because the roll will likely have the highest curvature near the hole of the membrane. With only one cut, the mirror can retain more stability than in the multi-cut packaging scheme, but it obviously loses some of the stability of the original, uncut mirror in the umbrella and rolled folding patterns. Also, the single cut mirror rolled around itself would easily return to its original shape when released into space without the need of such elaborate support systems as in the multi-cut model.

A matrix describing the usable surface of the aperture can be generated and then sent to the MTF. A generous width of 0.3 m was used to simulate the single radial cut for the MTF in order to estimate the maximum usable d.

The MTF's of the matrix of an aperture with overall diameter 10 m and inner diameters of 5 m and 5.3 m are shown in Figure 13. According to the MTF, a hole of diameter 5 m is acceptable, but black

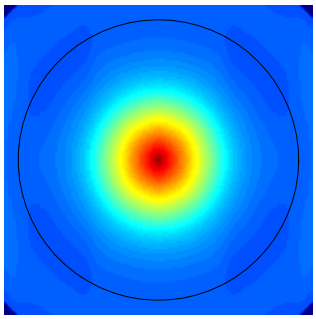

(a)

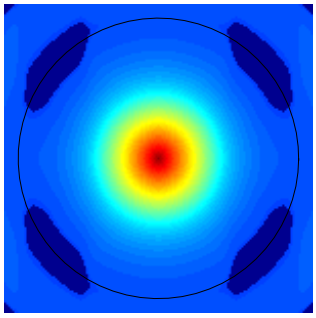

(b)

Figure 13: MTF of the aperture with $D = 10$ m and (a) $d = 5$ m, (b) $d = 5.5$ m.

spots appear within the circle of the MTF for a diameter of 5.3 m illustrating that this dimension is not feasible. A similar result is observed if $D = 20$ m and $d = 10$ m and $d = 10.7$ m, respectively. The maximum value of d for an aperture with a single cut appears to be close to $0.5D$ as noted previously. Hence, the single cut does not seem to greatly affect the MTF.

Although the actual mirror would probably retain a parabolic shape when rolled, estimates for the curvature of rolling the mirror are quite easy to compute when considering the overall shape as a cone. The original curvature of the mirror is ignored when considering different lengths in the geometry of the cone model (see Figure 14). To insure that the cone fits within the rocket, R_b (the radius of the base of the cone) can be set equal to R_{rocket}. Furthermore, R_t (the radius of the top of the cone) can be used as an estimate of the smallest radius of curvature in this packaging model. Thus it follows from properties of similar triangles that

$$\frac{R_t}{d} = \frac{R_{rocket}}{D}$$
$$ds \Rightarrow R_F \approx R_t = \tfrac{d}{D} R_{rocket}.$$

Hence, the maximum curvature of rolling the mirror around itself can be estimated using the known

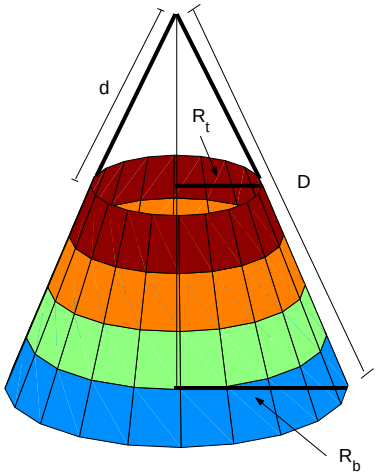

Figure 14: The geometry of the cone model.

constraint of rocket size, the diameter of the overall mirror, the diameter of the hole in the aperture found from the MTF, and simple geometry. Furthermore, the inside of the rocket has known radius $R_{rocket} = 2$ m, and an estimate for R_t can be computed using the results from the MTF. Hence, it follows that

$$\begin{aligned} R_t &\approx 2 \cdot \tfrac{d}{D} \\ &\approx 2 \cdot \tfrac{D/2}{D} = 1, \end{aligned}$$

Finally, we note that $R_F \approx 1$.

One could consider other single cut packaging methods, such as using a parabolic function instead of a cone or stretching the mirror out into more of a spiral. The parabolic idea does warrant more study, but a spiral wrapping scheme may require curvatures that are too large for presently accessible materials.

Discussion of Models

The estimated R_F values for various materials were computed using the relation

$$w \approx \left(\frac{t}{2R_F} \frac{E}{H} \right)^{\frac{1}{n}} \frac{\hat{D}^2}{4t},$$

from [1], where t is the thickness of the aperture, R_F is the radius of curvature of the folding model, E is the elastic modulus of the material, n is the strain hardening exponent, H is the plasticity model constant, $\hat{D}$ is the length of the surface being curved, and w is a measure of deflection. The value of w should be kept very low because the mirror will not reflect properly after even small deformations. As a

Table 2: Minimum allowable radii of curvature for different materials and different widths for the cylindrical roll, single cut, and multi-cut models.

thickness (t)	R_F for 2014-T6 Aluminum	R_F for I-400 Beryllium	R_F for 304 Stainless Steel
$10\mu m$	0.0012 m	557.3210 m	0.1187 m
$20\mu m$	0.0026 m	3340.2 m	0.2990 m
$30\mu m$	0.0040 m	9520.7 m	0.5135 m
$40\mu m$	0.0055 m	20018 m	0.7535 m
$50\mu m$	0.0069 m	35627 m	1.0147 m

Table 3: Minimum allowable radii of curvature for different materials and different widths for the umbrella model.

thickness (t)	R_F for 2014-T6 Aluminum	R_F for I-400 Beryllium	R_F for 304 Stainless Steel
$10\mu m$	0.0012 m	312.8706 m	0.1051 m
$20\mu m$	0.0025 m	1875.1 m	0.2648 m
$30\mu m$	0.0039 m	5344.8 m	0.4547 m
$40\mu m$	0.0053 m	11238 m	0.6673 m
$50\mu m$	0.0068 m	20000 m	0.8985 m

result, $w = 1\mu m$ was deemed an appropriate estimate of allowed deflection and was used to approximate the minimum R_F value (or alternatively, the maximum curvature, $1/R_F$) that the specific material can be shaped to hold without losing the necessary properties of the mirror. For the single cut and multi-cut models as well as the cylindrical roll model, $\hat{D}$ can be estimated by the circumference of the circle with highest curvature. Hence, in these models, $\hat{D} = 2\pi R_F$. The equation from [1] can then be rewritten to yield

$$w \approx \left(\frac{t}{2R_F}\frac{E}{H}\right)^{\frac{1}{n}} \frac{(2\pi R_F)^2}{4t}$$

$$\Rightarrow \left(\frac{4tw}{4\pi^2 R_F^2}\right)^n \approx \frac{t}{2R_F}\frac{E}{H}$$

$$\Rightarrow \left(\frac{(tw)^n}{\pi^{2n}}\right)\frac{2H}{Et} \approx R_F^{2n-1}$$

and therefore the minimum allowable radius of curvature can be computed using thickness and material properties. Using the outside loop of the umbrella base curve model, the value $D = \frac{5}{3}\pi R_F$ can be used to approximate the minimum allowed R_F for different materials by noting that

$$w \approx \left(\frac{t}{2R_F}\frac{E}{H}\right)^{\frac{1}{n}} \frac{(\frac{5}{3}\pi R_F)^2}{4t}$$

$$\Rightarrow \left(\frac{36tw}{25\pi^2 R_F^2}\right)^n \approx \frac{t}{2R_F}\frac{E}{H}$$

$$\Rightarrow \left(\frac{36tw}{25\pi^2}\right)^n \frac{2H}{Et} \approx R_F^{2n-1}.$$

Using these equations and material constants from [1], the minimum allowable radii of curvature for the single cut, multi-cut, and cylindrical roll models for different materials were computed and are summarized in Table 2 for various thicknesses of the aperture. Estimates for the minimum allowable radii of curvature for the umbrella model are contained in Table 3.

These values can be compared to the radii of curvature needed for each model to fit within the rocket to decide if each scheme is usable. As long as a particular R_F from the tables is smaller than the R_F needed for a model, that material at that thickness will work for the model being considered. For all apertures that are 10-50 μm thick, both aluminum and stainless steel appear to be feasible materials if using any of the presented models with appropriate choices for the number of cuts in the multi-cut model and for the number of folds in the umbrella model. Beryllium does not appear to be an appropriate material for the aperture, but the physical properties of beryllium make it a less than favorable choice for the mirror regardless of curvature. Adequate stability of the aperture can possibly be achieved simply by maximizing the thickness of the mirror within the

constraint that the radius of curvature of the model is larger than the radius of curvature allowed by the material.

Since the models are simplifications, physical testing is definitely necessary. Despite some of the simplifications with regard to original mirror curvature, all models presented do warrant the further study of physical models. The value for allowable deflection of the mirror w should also be thoroughly tested and may vary with material. Higher stability is achieved by higher natural frequency, and further study with these models with regard to natural frequency is suggested as well. Also, more research on possible support structures for the mirror would help the analysis of optimal mirror packaging.

Optical Considerations

When considering the packaging of a membrane, the spatial frequency response of the resulting aperture is a key performance factor. Assuming that the optical system is diffraction limited and contains no aberrations, one measure of the spatial frequency response is the modulation transfer function (MTF) given by [3]:

$$\aleph(f_x, f_y) = \frac{\iint P_1(\xi,\eta)P_2(\xi,\eta)\, d\xi d\eta}{\iint P(\xi,\eta)\, d\xi d\eta}$$

where

$$P_1(\xi,\eta) = P\left(\xi + \frac{\lambda d_i f_x}{2}, \eta + \frac{\lambda d_i f_y}{2}\right)$$

$$P_2(\xi,\eta) = P\left(\xi - \frac{\lambda d_i f_x}{2}, \eta - \frac{\lambda d_i f_y}{2}\right).$$

Here (ξ,η) are spatial variables in the 2-D plane, λ is the wavelength, P is the pupil function, and d_i is the distance to the image. The pupil function is a spatially-defined binary function which is identity whenever the aperture exists and is zero elsewhere. For example, a perfectly round primary mirror of radius two will have a cylindrical pupil function of radius one and height one.

The MTF for a diffraction-limited, aberration free system defines the spatial frequencies that can be resolved by such an optical system. Using the above equation and applying it to a circular aperture of diameter ℓ produces the MTF

$$\aleph(\rho) = \begin{cases} \frac{2}{\pi}\left[\cos^{-1}\left(\frac{\rho}{2\rho_0}\right) - \frac{\rho}{2\rho_0}\sqrt{1-\left(\frac{\rho}{2\rho_0}\right)^2}\right], \rho \le \rho_0 \\ 0\ , \text{ otherwise} \end{cases}$$

where

$$\rho_0 = \frac{\ell}{2\lambda d_i}\,.$$

For the above case, a one-meter aperture at a Low Earth Orbit of 500 km at a one-micron wavelength can resolve 1 cycle per meter of resolution. This value is the limiting aperture parameter being investigated. For most cases, an analytical solution is difficult to calculate and the MFT must be found computationally. The remainder of the analysis was performed computationally using Matlab.

When determining the minimal spatial frequency from the above example, noise has not been included in the analysis. Generally, it can be assumed that below some percentage of the peak MTF value, noise dominates the optical resonance and spatial information cannot be discerned. A value of 20% of the peak value was used this paper, with comparisons made to the ideal case shown above for a circularly filled aperture.

All of the previously mentioned packaging schemes were examed for impact to MTF performance. However, the multi-cut models [4] were found to be the most difficult to analyze with respect to MTF performance and had the most impact on optical performance. No circular symmetry exists and the potential gaps in the aperture could create effective zeros in the MTF. Therefore, only the multi-gap analysis is shown.

For the multi-cut MTF analysis, three variables were studied: obscuration size, number of cuts/gaps, and angle of the gap. Each cut was placed symmetrically and each cut angle was the same for each case.

Figures 15 and 16, respectively, illustrate the pupil function and the resulting normalized MTF for a six

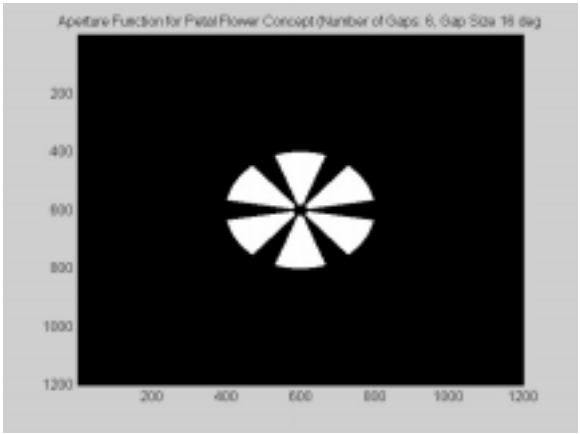

Figure 15: (a) Pupil function for 6-16 degree gap aperture with a 10% obscuration.

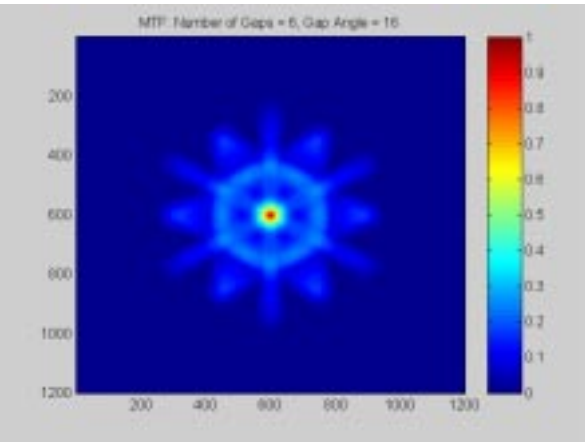

Figure 16: (a) MTF for Figure 15 pupil function.

16-degree multi-cut gap in the aperture with a 10% obscuration. For the pupil function, the white areas indicate where the pupil function is one while the black areas indicate areas where no aperture exists. The 10% obscuration in the middle was created to accommodate an on-axis secondary mirror. For this case, the spatial frequency cut-off was 84% of that for a circular aperture with no gaps or obscuration.

For the study, the number of gaps was varied from 5 to 10, while the angle of the gap was varied from 5 until no aperture existed. The dependent variable was the cut-off frequency divided by the cut-off frequency for completely filled aperture with no gaps or obscurations. Figure 17 shows the results of that study. For equally spaced and equal-angle gaps, the analysis showed a surprising trend – the gap angle and the number of gaps could be combined into one variable – the total radial gap angle. Figure 17 shows the results for an obscuration of 10%. As the obscuration increases, the curves half-bell-shape tended to narrow, with more pronounced drops in the spatial frequency percentage for smaller total gaps. In general, this is due to the increased lack of aperture in the center.

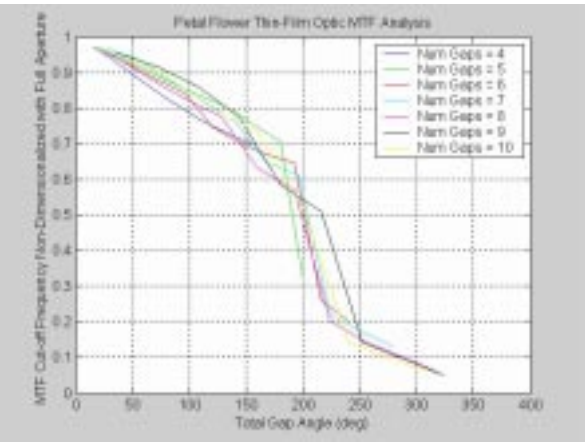

Figure 17: (a) MTF percentage as a function of completely filled aperture versus total gap angle (10% obscuration).

Acknowledgements

The Industrial Mathematics Modeling Workshop was supported by the National Science Foundation through the grant DMS-0204515 with additional support provided by the Center for Research in Scientific Computation (CRSC) and Department of Mathematics, North Carolina State University, and the Statistical and Applied Mathematical Sciences Institute (SAMSI).

References

[1] J.L. Domber and L.D. Peterson, "Implications of Material Microyield for Gossamer Optical Reflectors," 43rd Structures, Structural Dynamics and Materials conference, Denver, AIAA 2002-1503, April 2002.

[2] M.S. Lake, L.D. Peterson and M.B. Levine, "A Rationale for Defining Structural Requirements for Large Space Telescopes," 42nd Structures, Structural Dynamics and Materials conference, Seattle, AIAA 2001-1685, April 2001.

[3] J.W. Goodman, *Introduction to Fourier Optics*, McGraw-Hill, New York, NY, 1968.

[4] B. Tibbalds, S.D. Guest and S. Peligrino, "Folding Concept for Flexible Surface Reflectors," 39th Structures, Structural Dynamics, and Materials Conference and Exhibit, Long Beach, CA, AIAA98-1836, April 1998.